

EXPERIMENTAL APPROACH FOR EVALUATING EXHAUST FLOW DISTRIBUTION FOR PZEV EXHAUST MANIFOLDS USING A SIMULATED DYNAMIC FLOW BENCH

I. G. HWANG¹⁾, C.-L. MYUNG¹⁾, H. S. KIM²⁾ and S. PARK^{1)*}

¹⁾Department of Mechanical Engineering, Korea University, Seoul 136-701, Korea

²⁾School of Mechanical and Aerospace Engineering, Seoul National University, Seoul 151-742, Korea

(Received 9 July 2007; Revised 27 August 2007)

ABSTRACT—As current and future automobile emission regulations become more stringent, the research on flow distribution for an exhaust manifold and close-coupled catalyst (CCC) has become an interesting and remarkable subjects. The design of a CCC and exhaust manifold is a formidable task due to the complexity of the flow distribution caused by the pulsating flows from piston motion and engine combustion. Transient flow at the exhaust manifold can be analyzed with various computational fluid dynamics (CFD) tools. However, the results of such simulations must be verified with appropriate experimental data from real engine operating condition. In this study, an experimental approach was performed to investigate the flow distribution of exhaust gases for conventional cast types and stainless steel bending types of a four-cylinder engine. The pressure distribution of each exhaust sub-component was measured using a simulated dynamic flow bench and five-hole pitot probe. Moreover, using the results of the pitot tube measurement at the exit of the CCC, the flow distribution for two types of manifolds (cast type and bending type) was compared in terms of flow uniformity. Based on these experimental techniques, this study can be highly applicable to the design and optimization of exhaust for the better use of catalytic converters to meet the PZEV emission regulation.

KEY WORDS : Flow distribution, Exhaust manifold, CCC (Closed-coupled Catalyst), PZEV (Partial Zero Emission Vehicle), Flow uniformity

1. INTRODUCTION

As the emission regulations become more stringent worldwide, the research and development on techniques for reducing engine-out emission and advanced after-treatment will receive greater attention as an efficient means of meeting SULEV (Super Ultra Low Emission Vehicle) among car makers (Kim *et al.*, 2001). Moreover, in North America, PZEV (Partial Zero Emission Vehicle) technology research for engine combustion characteristics and exhaust after-treatment systems has been largely aimed at intensively reducing gasoline vehicle emission in recent years. Therefore, it is highly required that domestic automobile manufacturers should develop technologies to meet the PZEV regulation without delay. More than 80% of the total hydrocarbon (THC) emissions during the Federal Test Procedure (FTP)-75 driving cycle were emitted within the first two minutes, before the catalytic converter reaches light-off temperature. Therefore, a number of studies on various factors of engine combustion, after-treatment, and precise engine control

etc., have been carried out for cold start emission reduction. Included among the technologies for reducing cold start emission, are exhaust after-treatment systems, (such as thin wall catalysts), electrically heated catalysts (EHC), flow optimized exhaust manifolds, and stainless steel exhaust manifolds, which have proven to be quite effective in meeting legislation standards for vehicle pollutant emissions (Kidokoro *et al.*, 2003; Mueller-Haas *et al.*, 2003). In particular, it is recognized that the design optimization during the concept phase of a vehicle, as applied to the exhaust manifold and catalytic converter in terms of flow distribution, is highly effective in meeting the PZEV regulation with less costly design changes for implementation. Therefore, method for optimization of the exhaust flow and improvement of exhaust manifold flow are necessary in order to meet the severe emission regulations and guarantee the durability of exhaust systems (Persoons *et al.*, 2004; Aria-Garcia *et al.*, 2001). In order to improve the exhaust manifold flow, computational analysis should keep pace with experimental work so that the time and cost of development can be shortened. Although the flow distribution of the exhaust system can possibly be predicted by CFD, the effective-

*Corresponding author. e-mail: spark@korea.ac.kr

ness and precision of simulation results should be properly validated by various kinds of engine test data (Kim *et al.*, 2005; Kim *et al.*, 2002; Park *et al.*, 1998). Although measurements on a fired engine are clearly desirable for this purpose, it is very difficult and nearly impractical. Therefore, rig tests which can provide helpful information on exhaust flow characteristics in the CCC and exhaust manifold have begun to be adopted as an alternative. In this study, an experimental approach for assessing the exhaust flow distribution is carried out on a flow rig for a production type exhaust system. The objective of this study is two fold; First, it is necessary to setup a comprehensive method of simulating the actual flow from the engine exhaust using a flow rig and to apply this method to a production type exhaust system. Second, the method must assess the pressure drop characteristics and flow distribution for two types of exhaust systems with different exhaust manifolds. To this end, the simulated dynamic flow bench which was composed of a blower, cylinder head, and exhaust system of gasoline engine was designed, manufactured, and tested. The pressure drop characteristics for the exhaust sub-component was investigated by using the simulated dynamic flow bench. The pressure distribution at the outlet of the CCC was measured with five-hole pitot probe. Based on the quantitative data obtained from this fundamental experimental work, the flow distribution at the exit of the CCC was compared for two types of exhaust manifolds (cast type and bending type) in terms of flow uniformity.

2. TEST EQUIPMENT AND METHOD

2.1. Geometric Configuration of Exhaust Manifolds

The experimental apparatus used in this study was designed to measure exhaust pressure characteristics and the velocity profile at the catalyst outlet of the catalytic converter. Figure 1 shows the configuration of two types of exhaust manifolds used. The first one is conventional

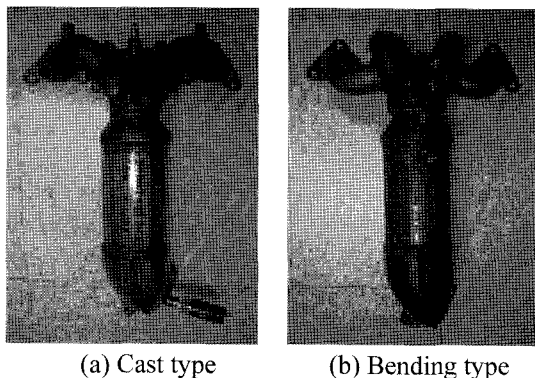


Figure 1. Exhaust manifold type.

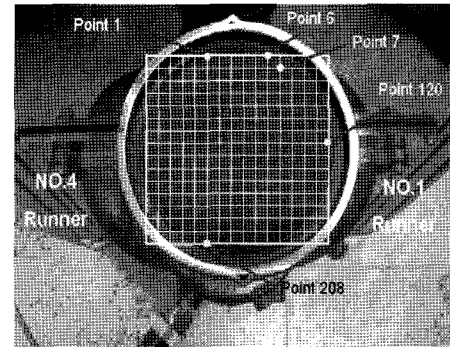


Figure 2. Flow analysis point on the CCC exit section.

Table 1. Specification of multi turbo blower.

Power source	60HZ
Power	25HP (18.5 kW)
Mass flow meter	3 m ³ /min
Maximum speed	5500 rpm
Diameter (Φ)	Suction : 100 mm Discharge : 100 mm

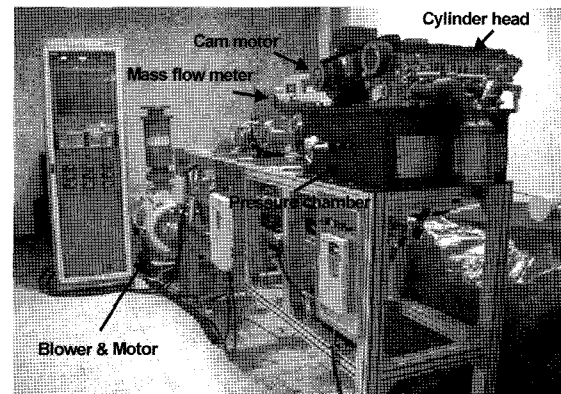


Figure 3. Simulated dynamic flow bench.

4-2-1 cast type and the second one is a stainless bending 4-1 type with a CCC. The stainless steel bending type is designed to improve light-off temperature during cold start. The engine displacement is 2.0 liters and the cell density of the CCC used is 900 cpsi/2.5 mil. Figure 2 represents the measurement points of exhaust flow at the exit section of the CCC. The No.1 runner of the exhaust manifold is located on the right side of catalyst in Figure 2.

2.2. Test Equipment

Figure 3 shows the schematics of the simulated dynamic flow bench. Detailed specifications for the blowing rig are shown in Table 1. The blowing rig was composed of multi turbo (which can supply an exact flow-rate with

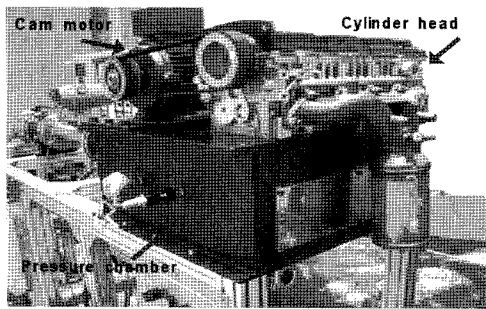


Figure 4. Simulated dynamic flow equipment using cylinder head.

specific engine operating condition), mass flowmeter, and surge tank of which function was minimized the flow and pressure fluctuation. In this research, the CCC with a cell density of 900 cpsi and an underfloor catalytic converter (UCC) with a cell density of 300 cpsi were used. To match the exhaust back pressure, an exhaust muffler system with the main muffler and sub-muffler of a production engine was adopted. Six pressure sensors were installed to measure the pressure drop across major sub-components of each exhaust system, and temperature sensors were set at the pressure chamber and the outlet of a main muffler. The simulated dynamic flow bench using a cylinder head is shown in Figure 4. A multi-cylinder engine head (2.0 liters) was located on the pressure damper. Lubricant oil is filled in the upper head side and circulated with the oil pump to reduce the mechanical friction between the cam shaft and valve-train.

The advantages of the dynamic flow bench are summarized as follows. As the valve-train of the real head is operated over 2000 rpm engine speed with motor, pulsating flow through the exhaust valves and ports can be generated and effectively supplied into the catalyst, while a steady flow bench cannot be uniquely realized. With the valve motion, the realistic exhaust flow characteristics through the cylinder head can be effectively simulated. In addition to this, steady flow testing at various valve lifts would be possible without operating the cylinder head. In conclusion, pulsating flow behavior as well as steady flow patterns during engine exhaust periods can be simultaneously simulated by adopting the dynamic flow rig.

Figure 5 shows the five-hole pitot probe system for calculating the pressure distribution at the exit of CCC monolith. Flow velocity at the catalyst monolith was measured with a pitot device installed after the CCC exit region. Pressure was measured with the a 9010 model of the pressure transmitter made by Pressure Systems Corporation. Three dimensional traverse with a spatial resolution of 0.1mm was used for the precise movement of the probe. In this study, definite 2-D spacing was

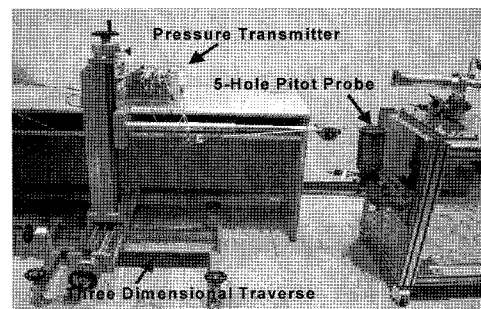


Figure 5. Five-hole pitot probe measurement system.

adopted to measure the flow velocity and pressure distribution at the exit of the CCC substrate.

2.3. Test Methods

Since the temperature of compressed air increases as the motor operates, intermittent flow analysis was performed at the specific temperature settling point of air. The maximum flow capacity of a 2.0 liter engine was equivalent to rated engine speed with this system. Mass flow rate can be expressed as a function of the engine speed, displacement, and volumetric efficiency of tested engine. The mass flow rate at 1000 rpm~5000 rpm ranges 14.5 L/s~80.4 L/s considering the volumetric efficiency of the tested engine.

$$Q(l/s) = \frac{N \times V_d \times \eta_v}{2 \times 60(\text{sec}) \times 1000(\text{cc/l}) \times 100} \quad (3)$$

Here, N : Engine speed (RPM)

V_d : Engine displacement (cc)

η_v : Volumetric efficiency (%)

Flow distribution between the exhaust manifold and catalyst section was influenced by the turbulent flow attributed to manifold geometry and valve mechanism. As the complex flow motion was generated over the exhaust manifold and diffuser before the catalyst, the following procedure was selected to quantify the flow distribution at the catalyst section.

It can be assumed that the exhaust flow just before the monolith of each channel passed through the catalyst outlet. The flow uniformity of a catalyst was analyzed using the velocity distribution at the outlet section of the substrate. The effect of flow around the outer wall of the catalyst was ignored in this research because the pitot

probe technique has some basic limitation in measuring the flow in the vicinity of a mat and catalyst canning due to the dimension of nominal probe diameter. The pitot probe was positioned about 5 mm away from the outer wall to avoid flow interference. The number of data acquisition points at the exit of the CCC substrates section was effectively set equal to 208 points, excluding

outer wall spacing and canning procurement. The measured pressure value of 208 points was corrected with a cubic spline in the compensation curve and the specific flow velocity on every grid was calculated using corresponding pressure coefficients.

In this study, Weltens' uniformity index was utilized for evaluating the flow distribution at the exit of the CCC for two types of exhaust manifolds (Weltens *et al.*, 1993). This can provide an overview of the uniformity of exhaust flow in terms of enhancing the conversion efficiency and even temperature distribution of a catalyst which is closely related to the durability of the catalyst.

$$\bar{\omega} = \frac{\sum \omega_i}{n} \tag{2}$$

$$\omega = \frac{1}{n} \sum \frac{\sqrt{(\omega_i - \bar{\omega})^2}}{\bar{\omega}} \tag{3}$$

$$\gamma = 1 - \frac{1}{2} \omega \tag{4}$$

Here, ω_i , $\bar{\omega}$, and n represent the velocity of the measuring point, mean velocity and cell numbers of the catalyst frontal surface. Finally, γ is defined as uniformity index of the catalyst.

The flow rate of the simulated bench was equivalent to 1000 and 2000 rpm cases of the tested engine. Though the engine has four cylinders, the maximum flow rate of each cylinder was supplied when the exhaust valves were fully open. In this case, the exhaust flow of the other cylinders can be easily excluded and a specific ports exhaust flow can be considered. Table 2 denotes the crank angle at which the exhaust valve of each cylinder opens at the ratio of 48, 68 and 100%. Figure 6 shows a

Table 2. Crank angle of the variable exhaust valve open ratio.

Ex. valve open	#1	#3	#4	#2
Crank angle	187	7	367	547
(No. 1 cylinder TDC: 0°CA)	203	23	383	563
	248	68	408	608

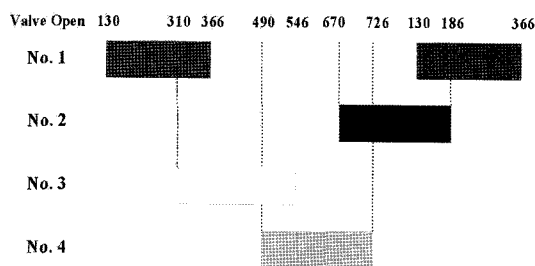


Figure 6. Exhaust valve open and closing time of each cylinder.

Table 3. Pressure difference data of cast type/bending type exhaust system (unit: kPa).

Position	1000 rpm	2000 rpm	3000 rpm	4000 rpm	5000 rpm
Total	2.8/2.9	8.5/8.9	15.3/15.8	22.7/23.2	30.6/31.2
CCC in	2.8/2.9	8.5/8.8	15.1/15.5	22.5/23.1	30.0/30.6
UCC in	1.2/1.7	5.3/5.9	10.1/10.6	15.8/15.9	20.8/21.0
Muf. in	1.0/1.5	4.65/5.5	8.6/9.5	13.1/13.4	16.6/17.9

diagram of the exhaust valve opening event (EVO BBDC 50°CA, EVC ATDC 6°CA) of the tested engine.

3. TEST RESULT AND DISCUSSION

3.1. Pressure Characteristics of the Exhaust Sub Components

3.1.1. Exhaust system pressure drop analysis

Table 3 shows the exhaust back pressure at each exhaust sub-component's locations with cast and bending type respectively. In this test, the cylinder head was not installed to allow comparison of the pressure drop of each manifold system. At the entrance section of the substrate, the pressure of bending type exhaust manifold at 2000 and 5000 rpm was 0.3 kPa and 0.6 kPa higher than that of the cast type manifold. In the case of main muffler inlet, the pressure difference is 0.75 kPa and 1.3 kPa higher with the bending type exhaust manifold at 2000 and 5000 rpm, respectively.

3.1.2. Pressure difference of each exhaust sub-component

Figures 7 and 8 show the pressure difference of each exhaust sub-component. In this case, only the exhaust manifold was changed, while other components such as UCC, sub- and main muffler remained unchanged. The pressure drop was measured at CCC, UCC and main muffler inlet/outlet position respectively. As shown in Figures 7 and 8, the main muffler has the highest pressure

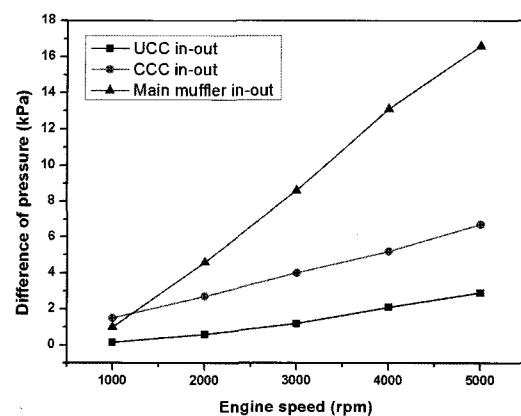


Figure 7. Pressure difference of cast type.

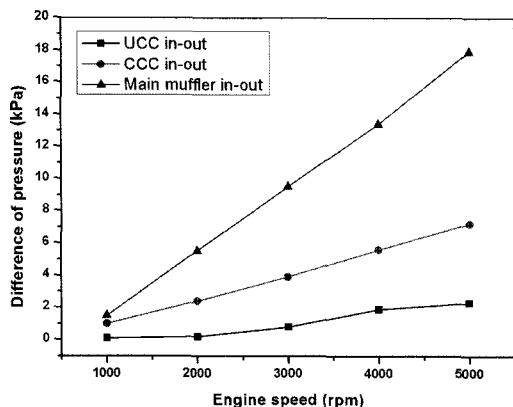


Figure 8. Pressure difference of bending type.

drop of 54.1% for cast type and 61.8% for bending type at 2000 rpm, while that of the CCC was 31.8% and 27.0%, respectively. The UCC has a minimum pressure increment whose level was 7.1% and 2.2%. This suggests that the main muffler plays an important role in lowering exhaust pressure and has influence on the maximum engine power.

However the back pressure increment of CCC accounts for 30% of total back pressure in the tested exhaust system. This means that the flow optimization of the exhaust manifold would be needed to guarantee the development of a high-performance and low-emission engine.

3.2. Flow Analysis at the Exit of CCC Section

3.2.1. Exhaust flow distribution at 1000 rpm

Figure 9 shows the velocity distribution at the exit section of CCC for a cast type exhaust manifold in the case of 1000 rpm condition. From this figure, the ratio of exhaust valve opening is 68% and flow area is a maximum value. Figure 9(a) shows flow distribution at the exhaust valve opening of the #1 cylinder. As shown in the Figure 9(a), exhaust flow from the #1 cylinder was directed to the upper right-hand section of the catalytic substrate. The average velocity at the upper right section is 4.75 m/s, and the velocity at the other section ranges between 3.67 and 4.0 m/s. The increase in average velocity on the upper right side is about 19~24.3%. Figure 9(b) shows flow distribution at the exhaust valve opening of the #2 cylinder only. Similar to Figure 9(a), the flow is directed towards the upper right side of the substrate. It is caused by the geometric configuration of the exhaust manifold. The 2nd runner joined with the 1st runner at the lower section of 1st runner. On the contrary, the average velocity of the lower left side of the catalyst is higher than at the other section, as shown in the Figure 9(c). In Figure 9(d), flow velocity of the upper left section has the highest value. This is the condition at the exhaust valve opening of the #4 cylinder. It can be explained by the fact

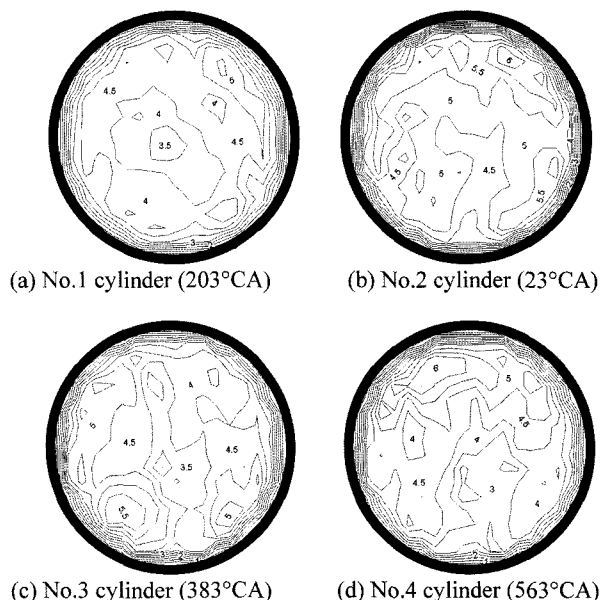


Figure 9. Flow distribution in cast type at 1000 rpm.

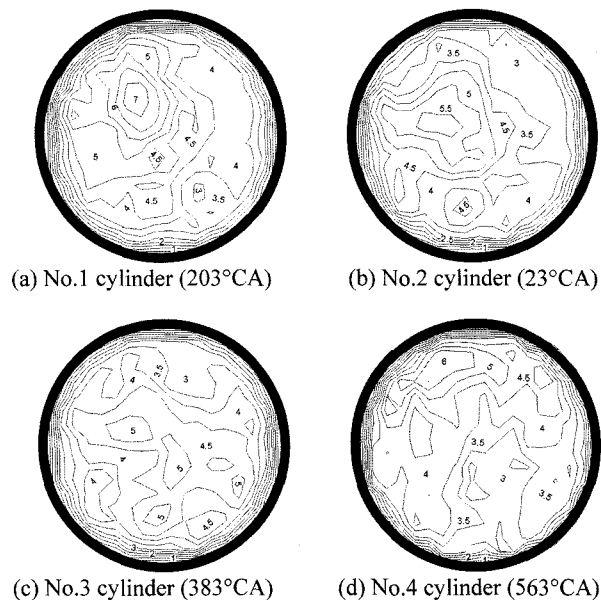


Figure 10. Flow distribution in bending type at 1000 rpm.

that the geometric configuration of the cast type manifold is symmetric.

Figure 10 shows the velocity distribution at the exit section of the CCC for the bending type exhaust manifold in the case of the 1000 rpm condition. Exhaust flow from the 1st and 4th cylinder is concentrated on the upper side section of the CCC exit section. The main flow from the 2nd and the 3rd runners is concentrated on the center part of the CCC exit section. The deviation of average velocity in the bending type is relatively higher than that of

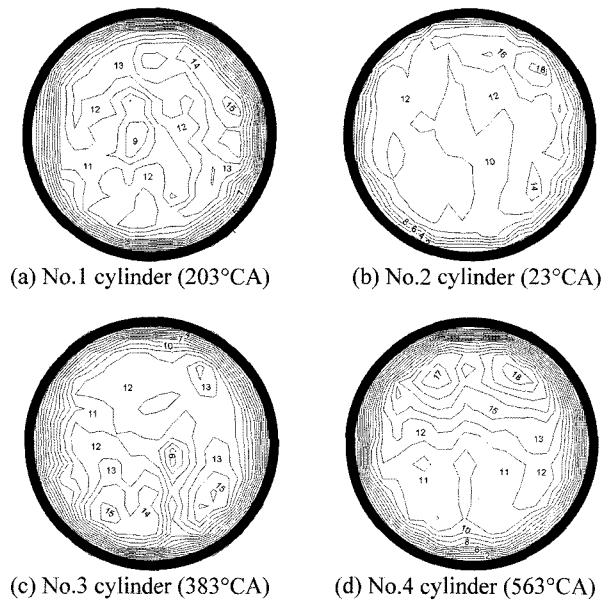


Figure 11. Flow distribution in cast type at 2000 rpm.

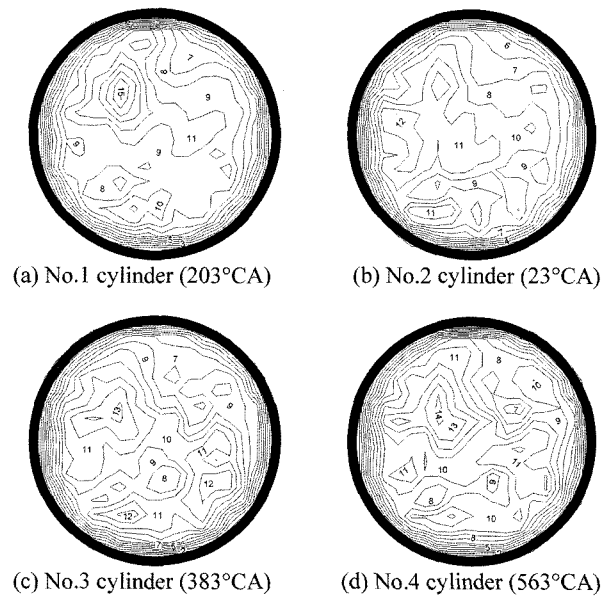


Figure 12. Flow distribution for bending type at 2000 rpm.

the cast type. Thus, the deterioration in flow uniformity index can cause.

3.2.2. Exhaust flow distribution at 2000 rpm

Figures 11 and 12 show the velocity distribution at the exit section of the CCC for two types of exhaust manifolds at the 2000 rpm operating condition. Flow distribution is very similar to the 1000 rpm condition. The deviation of velocity magnitude in the bending type is also higher than that of cast type.

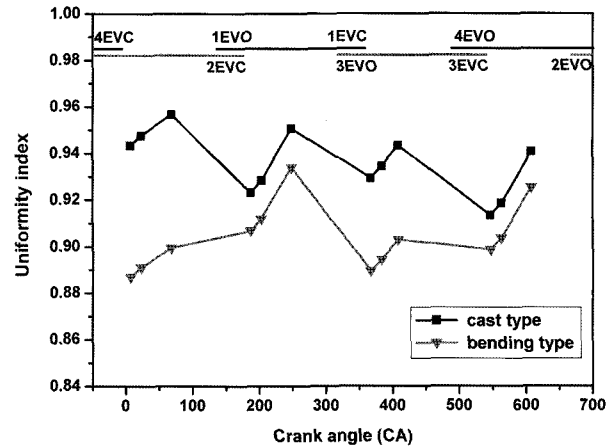


Figure 13. Uniformity index at 1000 rpm.

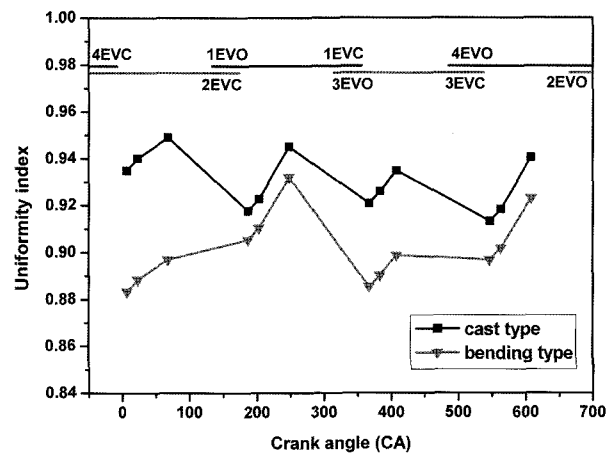


Figure 14. Uniformity index at 2000 rpm.

3.3. Comparison of Uniformity Index

Figures 13 and 14 show the uniformity index for two types of exhaust manifolds at the 1000 and 2000 rpm conditions. As shown in Figure 13, the arithmetic average uniformity for cast and bending type is 0.9358 and 0.9038 respectively. The uniformity index of the bending type is lower by 0.032 than that of the cast type. At the 2000 rpm condition in Figure 14, the arithmetic average uniformity of each type is 0.9303 and 0.9011, respectively. As in the case of the 1000 rpm condition, the uniformity index for the bending type is lower than that of the cast type. Also, it is also found that as engine speed increases, the uniformity index gets smaller. This is due to the fact that the velocity magnitude of the main flow which directs some part of the CCC outlet increases with engine speed.

4. CONCLUSIONS

In this research, the pressure distribution at the catalyst

outlet was measured on simulated dynamic flow bench. A pitot probe was used to measure the exhaust flow distribution at the exit of the CCC to quantify the flow uniformity for two types of exhaust manifolds. The major findings obtained from this study can be summarized as follows.

- (1) The exhaust pressure increment of the bending type is 0.3 kPa and 0.6 kPa higher than that of the cast type at the 1000 and 2000 rpm cases, respectively. This means that an engine power drop will be expected under the high load or high speed engine operating conditions in the case of the bending type exhaust manifold.
- (2) The primary exhaust flow of the bending type was headed to the diffuser wall and outside of the catalyst. This means that the exhaust flow uniformity of the bending type gets worse compared to the cast type. In order to improved the flow distribution at the catalyst inlet side, geometric modifications on the each manifold would be required.
- (3) The arithmetic average uniformity of the cast and bending types are 0.9358 and 0.9038, respectively. The uniformity index of the bending type is 0.032 smaller than that of the cast type. At the 2000 rpm condition, the arithmetic average uniformities of each type are 0.9303 and 0.9011, respectively. The uniformity index for the two types of exhaust manifolds is over 0.9, which is relatively high. It is thought that this leads to improvement of conversion efficiency and increases the life of converter system.
- (4) It is expected that the experimental approach derived from this study can be a useful tool to contribute to assuring the reliability of exhaust system and lead a substantial reduction in the development period for the exhaust after-treatment systems.

ACKNOWLEDGEMENT—This study is supported by Ministry of Commerce, Industry and energy, Hyundai Motor Company and Brain Korea 21 Project.

REFERENCES

- Arias-Garcia, A., Benjamin, S. F., Zhao, H. and Farr, S. (2001). A comparison of steady, pulsating flow measurements and CFD simulations in close coupled catalysts. *SAE Paper No.* 2001-01-3662.
- Kidokoro, T., Hoshi, K., Hiraku, K., Satoya, L., Watanabe, K., Fujiwara, T. and Suzuki, H. (2003). Development of PZEV exhaust emission control system. *SAE Paper No.* 2003-01-0817.
- Kim, D., Kwak, H. and Park, S. (2005). Flow analysis with CFD on the exhaust manifolds for PZEV. *Spring Conf. Proc., Korean Society of Mechanical Engineers*, 3112–3117.
- Kim, H. S., Min, K., Myung, C. L. and Park, S. (2002). A combined experimental and computational approach to improve catalyst flow uniformity and light-off behavior. *Proc. Instn. Mech. Eng.*, **216**, Part D: *J. Automobile Engineering*, 413–430.
- Kim, I. T., Lee, W. J., Yoon, J. S. and Park, C. K. (2001). An exploratory study of THC emission reduction technologied compliant with SULEV regulations. *Int. J. Automotive Technology* **2**, **2**, 63–75.
- Mueller-Haas, K., Brueck, R., Rieck, J. S., Webb, C. C. and Shaw, K. A. (2003). FTP and US06 performance of advanced high cell density metallic substrates as a function of varying air/fuel modulation. *SAE Paper No.* 2003-01-0819.
- Park, S. B., Kim, H. S., Cho, K. M. and Kim, W. T. (1998). An experimental and computational study of flow characteristics in exhaust manifold and CCC (Closed-Coupled Catalyst). *SAE Paper No.* 980128.
- Persoons, T., Van den Bluck, E. and Fausto, S. (2004). Study of pulsating flow in close coupled catalyst manifolds using phase-locked hot-wire anemometry. *Exp. Fluids* **36**, **2**, 217–232.
- Weltens, H., Bressler, H., Terres, F., Neumaier, H. and Rammoser, D. (1999). Optimization of catalytic converter gas flow distribution by CFD prediction. *SAE Paper No.* 930780.